3 Biotech (2020) 10:427
https://doi.org/10.1007/s13205-020-02401-3

ORIGINAL ARTICLE

Efficacy of chelerythrine against dual-species biofilms of *Staphylococcus aureus* and *Staphylococcus lugdunensis*

Weidong Qian[1] · Zhaohuan Sun[1] · Yuting Fu[1] · Min Yang[1] · Ting Wang[1] · Yongdong Li[2]

Received: 9 March 2020 / Accepted: 17 August 2020 / Published online: 11 September 2020

Abstract

Staphylococcus aureus and *Staphylococcus lugdunensis* are often associated with pathogenic biofilms ranging from superficial mucosal to life-threatening systemic infections. Recent studies have reported that chelerythrine (CHE) displays antimicrobial activities against a few microorganisms, but its effects on dual-species biofilms of *S. aureus* and *S. lugdunensis* have never been reported. The purpose of this study was to investigate how dual-species biofilms of *S. aureus* and *S. lugdunensis* respond when challenged with CHE. Minimum inhibitory concentration (MIC) of CHE against planktic cells in dual-species culture was 8 µg/mL. CHE also suppressed dual-species biofilm formation at minimal biofilm inhibitory concentration ($MBIC_{90}$, 4 µg/mL). Further, confocal laser scanning microscope (CLSM) using five fluorescent dyes revealed the dose-dependent reduction of the levels of three key biofilm matrix components, and reduced tolerance to gatifloxacin, of biofilms exposed to CHE. Moreover, CHE efficiently eradicated preformed dual-species biofilms at minimal biofilm eradication concentration (MBEC, 256 µg/mL). Hence, CHE has the potential to address biofilm infections of clinical course and other biofilm-related diseases caused by *S. aureus* and *S. lugdunensis*.

Keywords *Staphylococcus aureus* · *Staphylococcus lugdunensis* · Chelerythrine · Dual-species biofilm · Antibiofilm activity

Introduction

S. aureus, a ubiquitous bacterium, is a major human pathogen that resides in the skin and nasal membranes, and can frequently be found in raw, pasteurized milk and other food products (Dai et al. 2019; Tong et al. 2015). Its presence in the normal microbiota notwithstanding, its pathogenic potential is dreadful, and can cause various infections, from bacteremia and infective endocarditis as well as osteoarticular, pleuropulmonary, to hospital-acquired infections (Tong et al. 2015). It is also notable for its ability to produce various toxins and invasive enzymes. Similarly, *S. lugdunensis*, a coagulase-negative staphylococcus, is a skin commensal, but can also be responsible for nosocomial and community-acquired infections that clinically resemble those caused by *S. aureus* in terms of the virulence of the organism and the clinical course of infection (Frank et al. 2008). In addition, *S. lugdunensis* has been demonstrated to be involved in severe infections such as breast abscesses, peritonitis, infected joint prostheses, osteomyelitis, discitis, septic arthritis, and pacemaker infections (Van der Mee-Marquet et al. 2003).

Although single-species infections are sometimes seen, mixed bacterial biofilms are identified more frequently. Notably, *S. aureus* and *S. lugdunensis* are common causative agents of infections associated with medical devices because of their capacity to adhere to the smooth surface of these materials, and to form a biofilm (de Oliveira et al. 2016). Furthermore, they are often found in other mixed species biofilm-related infections (Shin and Eom 2019; Lee et al. 2019).

Biofilms are composed of cells in a sessile state, held together by a physical scaffold with a matrix of extracellular polymeric substances (Hobley et al. 2015). Bacteria in biofilms are intrinsically resistant to antimicrobials, host immune response, and biocides, and bacteria living in

✉ Weidong Qian
qianweidong@sust.edu.cn

[1] Department of Pharmacy, Food Science and Bioengineering College, Shaanxi University of Science and Technology, Xi'an 710021, People's Republic of China

[2] Ningbo Municipal Center for Disease Control and Prevention, Ningbo 315010, People's Republic of China

biofilms can be up to 1000-fold more antibiotic-resistant than planktonic cells of the same microorganism (Olson et al. 2002). It is well recognized that biofilm-related infections are extremely difficult to treat successfully. However, there are many plant-derived products with reported antibacterial, antifungal, antioxidant, and anti-inflammatory properties that may have the potential to address biofilm-related infections (Rashed et al. 2014).

Chelerythrine (CHE, Fig. 1), a potent and widely used broad-range, cell-permeable protein kinase C inhibitor, is a natural benzophenanthridine alkaloid which has shown anti-cancer effects on various types of human cancer cells (Yang et al. 2012). In addition, CHE has multiple other pharmacological activities, including anti-bacterial, anti-inflammatory, insecticidal, and anti-fibrosis activities. For instance, it has been reported that CHE has strong antibacterial activities against gram-positive *S. aureus*, methicillin-resistant *S. aureus*, and extended-spectrum-β-lactamase-producing *S. aureus*. The study showed CHE Minimum inhibitory concentrations (MICs) of 156 μg/mL against each of three bacterial species (He et al. 2018). However, no studies have been performed to clarify the effects of CHE against *S. aureus*-*S. lugdunensis* mixed-species biofilms. In this work, we investigated the ability of CHE to inhibit mixed-species biofilm formation, biofilm adhesion, and preformed biofilm.

Materials and methods

Reagents

CHE (CAS: 34316-15-9) was obtained from Nanjing DASF Biological Technology Co., Ltd. (Nanjing, Jiangsu, China) at an HPLC purity of at least 98%. Sample solution was prepared in dimethyl sulfoxide (DMSO) and sterilized by filtration immediately before use. Film tracer SYPRO Ruby (SYPRO Ruby), wheat germ agglutinin conjugated with Alexa Fluor™ 488 Conjugate (WGA), and 4′, 6-diamidino-2-phenylindole (DAPI) dyes were purchased from Invitrogen (Thermo Fisher Scientific, Waltham, MA, USA). All other chemicals were of analytical grade and were used as-received.

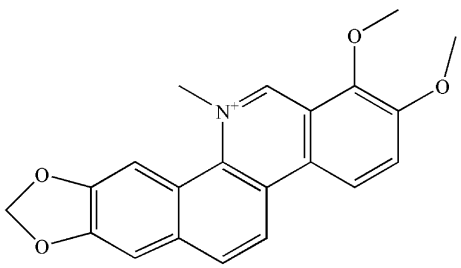

Fig. 1 The structure of chelerythrine

Bacterial strains and culture conditions

S. aureus ATCC 25,923 and *S. lugdunensis* ATCC 700,328 isolates were gifted by Dr. Yongdong Li (Ningbo, China), and stored in tryptic soya broth (TSB) with 20% glycerol (v/v) at – 80 ℃. Before each experiment, stock cultures were streaked on tryptic soya agar (TSA) and grown at 37 ℃ for 18 h. A loopful of each strain was then inoculated into 30 mL TSB and incubated in a shaking incubator overnight at 37 ℃ with constant shaking at 160 rpm.

Minimum inhibitory concentration (MIC) determination

The MIC of CHE against the single and dual-species cultures of *S. aureus* ATCC 25,923 and *S. lugdunensis* ATCC 700,328 described above were measured using the agar dilution method as reported previously (Shi et al. 2016). CHE was mixed with warm (50 ℃) melted TSA in a 24-well plate to achieve a concentration of 64 μg/mL. The mixture was further, continuously, twofold-diluted with melted TSA. The final concentrations of CHE ranged from 0 to 64 μg/mL. Samples to which only DMSO was added were used as a control group. After mixing, each well containing TSA and various concentrations of CHE, was inoculated with 2 μL of bacterial suspension. Tested bacteria were spotted and the plates were incubated at 37 ℃ for 24 h. The MIC was defined as the lowest concentration of CHE that allowed no visible growth of tested bacteria on agar plates.

Adhesion assay

To assess the primary cell-surface interaction, an adhesion assay was executed in a 24-well microtiter plate, as previously described (Shin and Eom 2019). Briefly, the final concentration of bacterial inoculum in TSB medium was adjusted to 1×10^6 CFU/mL. Cells supplemented with CHE at different concentrations (0, 1/8, 1/4, and 1/2 MIC) were then grown on the slides in a 24-well microtiter plate at 37 ℃ for 2 h. Subsequently, the supernatants were removed from the wells, and each well was slowly rinsed with 10 mM phosphate buffered solution (PBS) to remove non-adherent cells. Thereafter, adherent cells on the slides was incubated with SYTO 9 and propidium iodide (PI), and cultured in the dark for 15 min. The adherent cells were then evaluated by confocal laser scanning microscopy (CLSM).

Biofilm analysis by crystal violet staining assay (CVSA)

CVSA was performed as described by Guo et al. with a few modifications (Guo et al. 2019). In brief, single and dual-species cultures of *S. aureus* and *S. lugdunensis* were treated with CHE at different concentrations (1/16, 1/8, 1/4, 1/2, and 1 MIC) in a 96-well plate at 37 ℃ for 24 h, respectively. After treatment, nonadherent bacterial cells were removed by gently washing the wells with PBS three times, and then fixed with 100% methyl alcohol for 15 min. The biofilms on the microplate bottoms were stained with 200 µL of 0.1% crystal violet for 5 min and then washed with PBS to remove residual dye, followed by 95% ethanol for 30 min. The absorbance of released crystal violet (CV) in ethanol was recorded optical density at 575 nm by a microplate reader (Thermo Fisher Scientific, Finland).

Biofilm formation analysis

The effects of CHE on biofilm formation were evaluated qualitatively by CVSA, CLSM, and environmental scanning electron microscopy (ESEM, Q45, FEI, USA), as described by Qian et al., with minor modifications (Qian et al. 2019). Briefly, cell suspensions ($OD_{600}=0.5$) were grown in TSB with CHE concentrations at 0, 1/8, 1/4, and 1/2 MIC on round glass slips in a 24-well microtiter plate, followed by incubation at 37 ℃ for 24 h. The coupons with biofilm cells were kept in distilled water containing 2.5% glutaraldehyde at − 4 °C for 4 h and washed three times with 10 mM PBS. For CVSA analysis, the biofilms on the slips were stained with CV as described above and observed with an optical microscope. For CLSM analysis, the slides with biofilms were incubated with 2.5 µM SYTO 9 and cultured at 25 °C for 15 min. CLSM examination was performed with fluorescence measured at excitation/emission wavelengths of 485/542 nm for SYTO 9. For ESEM analysis, the samples were dehydrated in sequentially graded ethanol (50%, 70%, 90%, and 100%). Dehydrated biofilm samples were coated with gold with an ion-sputtering instrument before being observed by ESEM.

Gatifloxacin diffusion within biofilms treated with CHE

Diffusion of antibiotics within biofilms formed in the presence of CHE was performed with gatifloxacin possessing intrinsic fluorescence, and evaluated by CLSM (van der Waal et al. 2017). Dual-species biofilms were prepared in the same manner as described above on glass coverslips placed inside a 24-well microtiter plate. The resulting biofilms were gently washed three times with 10 mM PBS and a final concentration of 0.08 mg/mL gatifloxacin was added, followed by a further incubation for 5 h at 37 °C. Next, to visualize the diffusion of gatifloxacin within biofilms, SYTO 9 was added to the sample to a final concentration of 3 µM, followed by incubation for 15 min in the dark. The samples were then rinsed three times with 10 mM PBS to remove nonpenetrated gatifloxacin and observed using CLSM. The emission peak for gatifloxacin was recorded at 495 nm upon excitation at 291 nm.

Biofilm composition by CLSM

CLSM was used to examine compositional changes of *S. aureus*-*S. lugdunensis* dual-species biofilms (Oniciuc et al. 2016). Briefly, cells exposed to different concentrations of CHE (0, 1/4, and 1/2 MIC) were grown on a 24-well microtiter plate at 37 ℃ for 24 h. Following the incubation, bacterial suspensions were removed and rinsed with PBS. Thereafter, the biofilms were exposed to the following three types of dyes: (I) SYPRO Ruby, which labels most classes of proteins; (II) WGA, which stains *N*-acetyl-D-glucosamine residues; (III) DAPI, which binds to double-stranded DNA. At the end of each staining, the stained biofilms were washed with PBS to remove dye residues. All the staining steps were performed in the dark. The fluorescence of dyes was detected using the following combination of laser excitation and emission band-pass wavelengths: 450/610 nm for SYPRO Ruby (red), 495/519 nm for WGA (green), and 358/461 nm for DAPI (blue). ZEN software (Carl Zeiss, Thornwood, NY, USA) was used to observe the stained dual-species biofilm and to obtain color confocal images.

Evaluation of cell damage within biofilms

Cell damage within the dual-species biofilms was examined by CLSM as described by a previous study with slight modifications (Olszewska et al. 2019). Cells grown on slides at 37 ℃ for 48 h were cultured and then exposed to CHE at different concentrations (0, 2, 4, and 8 MIC) for 12 h, then washed three times with 0.9% NaCl. To observe the damage of cells within biofilms, a combination of SYTO 9, and PI fluorescent dyes were mixed thoroughly with biofilm-associated cells in the dark for 15 min at 25 ℃, followed by assessment of cell damage by CLSM.

Minimal biofilm eradication concentration

To test the potential ability of CHE to eradicate preformed mono and dual-species biofilms, a biofilm eradication assay was carried out in a 24-well microtiter plate as described by Meira Ribeiro et al., with some modifications (Ribeiro et al. 2015). Biofilms were pre-formed for 48-h on the glass slips in each well and then treated with CHE at different concentrations (0, 8, 16, and 32 MIC) for 12 h at 37 °C. The

biofilms were then observed using an ESEM. Meanwhile, the biofilm biomass was measured using a crystal violet staining assay.

Statistical analysis

All experiments were performed in triplicate. Statistical analyses were performed using SPSS software (SPSS 8.0 for Windows). The data are presented as the mean ± SD ($n = 3$). Differences between means were evaluated by Student's t test and defined as significant at $P \leq 0.01$.

Results

MIC of CHE against single and dual culture of *S. aureus* and *S. lugdunensis*

CHE presented an obvious inhibitory effect against mono- and dual-species culture of *S. aureus* ATCC 25,923 and *S. lugdunensis* ATCC 700,328 (Table 1). The MICs of CHE against *S. aureus* ATCC 25,923 and *S. lugdunensis* ATCC 700,328 were all 4 μg/mL. Besides, the MIC value of CHE against dual-species was 8 μg/mL.

Table 1 Minimum inhibitory concentrations (MIC, μg/mL) of Chelerythrine against single- and dual-species of *S. aureus* and *S. lugdunensis*

Strains	MICS (μg/mL)	MBIC90S (μg/mL)
S. aureus ATCC 25,923	4	2
S. lugdunensis ATCC 700,328	4	2
Dual-species	8	4

Inhibition of initial cell-surface interaction

CLSM was utilized to examine the inhibitory effect of CHE against the initial cell-surface interaction between *S. lugdunensis* and *S. aureus*. Following the adhesion phase (Fig. 2), increased concentrations of CHE clearly inhibited the adhesion of *S. lugdunensis* and *S. aureus*. Compared with the control, a CHE concentration of 1/2 MIC significantly suppressed adhesion. These results indicate that CHE intervened with the initial cell-surface interaction between *S. lugdunensis* and *S. aureus*, thus inhibiting biofilm formation.

A combination of crystal violet staining, CLSM, and ESEM assays suggests the inhibitory effect of CHE on biofilm formation

To determine whether CHE inhibited the biofilm formation without bactericidal effects, we grew biofilms supplemented with CHE at different concentrations. As shown in Fig. 3, the addition of CHE clearly reduced the relative biomass of mono- and dual-species biofilms in a concentration-dependent manner. When mono-species of *S. aureus* and *S. lugdunensis* exposed to CHE at the 1/4-MIC and 1/8-MIC, respectively, there is a significant difference in the relative biomass of biofilm compared with untreated group ($p < 0.01$). In contrast, the relative biomass of dual-species biofilms was significantly different between 1/4-MIC-CHE-treated and untreated groups ($p < 0.01$). The biomass was further down-regulated significantly ($p < 0.001$) after exposure to CHE at 1/2 MIC or MIC compared to the untreated control. These results show that CHE has an excellent inhibitory effect on biofilm formation, and $MBIC_{90s}$ of CHE against *S. aureus* and *S. lugdunensis* mono-species biofilms were 2 μg/mL, while the $MBIC_{90}$ of CHE against dual-species biofilms was 4 μg/mL (Table 1).

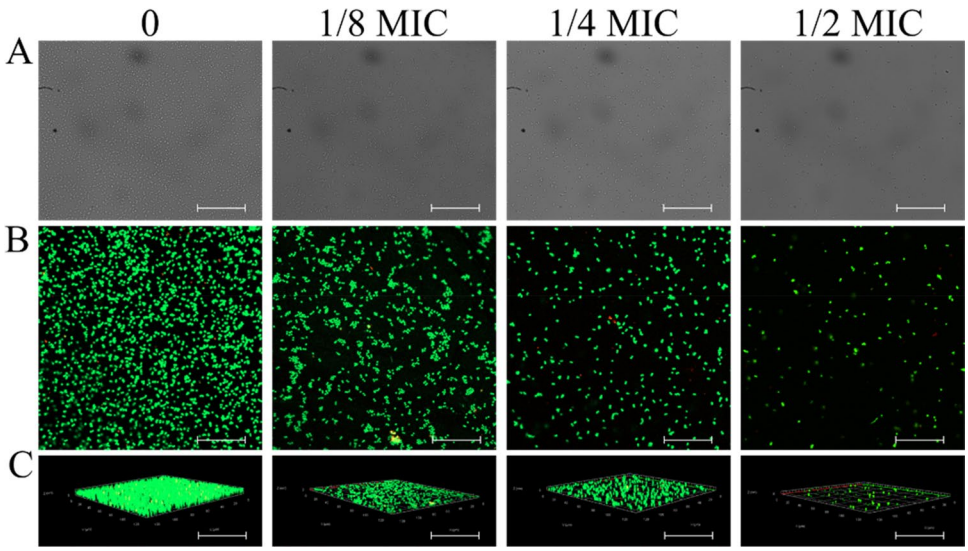

Fig. 2 Inhibitory effects of chelerythrine on initial cell surface interaction. **a** Images of confocal laser scanning microscopy (CLSM) of white light (scale bar: 20 μm). **b** Images of CLSM of fluorescence (scale bar: 10 μm). **c** Images of CLSM of fluorescence of three dimensional view (scale bar: 10 μm)

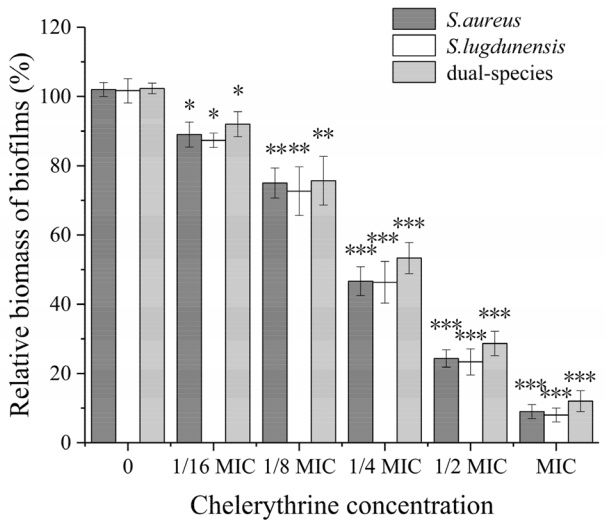

Fig. 3 Effects of chelerythrine on biofilm formation of mono- and dual-species of *S. aureus* ATCC 25,923 and *S. lugdunensis* ATCC 700,328. Relative biomass of biofilms was determined in the presence of chelerythrine at the concentrations of 0, 1/16 MIC, 1/8 MIC, 1/4 MIC, 1/2 MIC and MIC in 96-well plates by crystal violet staining. Values represent the means of triplicate measurements. Bars represent the standard deviation ($n=3$). *$P<0.05$; **$P<0.01$; ***$P<0.001$

Figure 4a, d and g display 40-fold-magnified optical microscopy images of biofilms stained with CV. The biofilm of *S. aureus* mono- and dual-species was efficiently restrained by CHE at 1/2 MIC, compared with the untreated group (Fig. 4a, g). However, biofilms of *S. lugdunensis* ATCC 700,328 were inhibited by CHE at concentrations of 1/4 MIC (Fig. 4d). The reduction of biofilm formation by CHE at sub-MIC was also observed using CLSM and ESEM (Fig. 4b, c, e, f, h, i). Examination of the of biofilms exposed to CHE indicated a dramatic reduction in the amount of biofilm biomass attached to the coverslip surface after CHE treatment, with fewer multilayer cell clusters.

CHE treatment reduces biofilms' tolerance to gatifloxacin

To evaluate the antibiotic tolerance of biofilms exposed to CHE, gatifloxacin diffusion within biofilms was comparatively monitored using CLSM. As shown in Fig. 5, in untreated or 1/8-MIC-CHE-treated biofilms, we observed that gatifloxacin was confined to the outer periphery of the biofilm with minimal to no penetration into the biofilm. By comparison, increased gatifloxacin penetration was found in the 1/4-MIC-treated group, and penetration was complete in the 1/2MIC-CHE-treated group, reaching the basal layers.

CHE suppressed biofilm formation by mediating extracellular proteins, polysaccharides, and eDNA levels

We used CLSM in conjugation with three different fluorescent dyes to quantify the levels of biofilm matrix components in dual-species biofilms in the presence of CHE. CLSM images showed that CHE significantly reduced biofilm polysaccharides, extracellular proteins, and eDNA in a dose-dependent manner (Fig. 6). These results were consistent with the decrease of total biofilm biomass following exposure to CHE. In the untreated group, substantial fluorescent emission overlap and large amounts of eDNA, proteins, and polysaccharides were observed, while only small clusters of bacteria and only a few fluorescent overlaps were evident in three main biofilm matrices in the 1/4-MIC-CHE-treated group. With 1/2 MIC, the three biofilm matrices were overtly attenuated, and scattered co-aggregation was reduced compared to the other groups.

CLSM showed inactivation by CHE of cells within dual-species biofilms

We also visualized stained biofilms by CLSM to investigate the effect of CHE on the viability of cells encased in biofilms. Live cells were stained with SYTO 9 (green), and PI (red) stained dead cells (Fig. 7). CHE had a dramatically detrimental impact on cell viability within biofilms and caused significant dispersion of cells within the biofilm matrix. The control samples untreated with CHE stained entirely in fluorescent green, reflecting intact cytomembranes or cell walls in live bacteria. By comparison, the experimental samples treated with CHE and showed a large percentage of fluorescent red with a small proportion of fluorescent green, demonstrating extensive bacterial damage. With 8 MIC CHE, images were almost entirely red, though there were patches that remained green, suggesting that some cells in these biofilms were still intact and viable.

CHE eradicated efficiently preformed biofilms

We used a crystal violet staining assay and ESEM to confirm the biofilm-eradicating potential of CHE at different concentrations. The biofilm biomass of *S. aureus* mono- and dual-species was significantly reduced by treatment with CHE at 32 MIC ($p<0.001$), while a similar result was achieved at 16 MIC in mono-species group of *S. lugdunensis* ($p<0.001$) (Fig. 8a). Effects observed at other CHE dosage levels confirmed this dose–response correlation (Fig. 8b–d). These results were consistent with those obtained using CVSA.

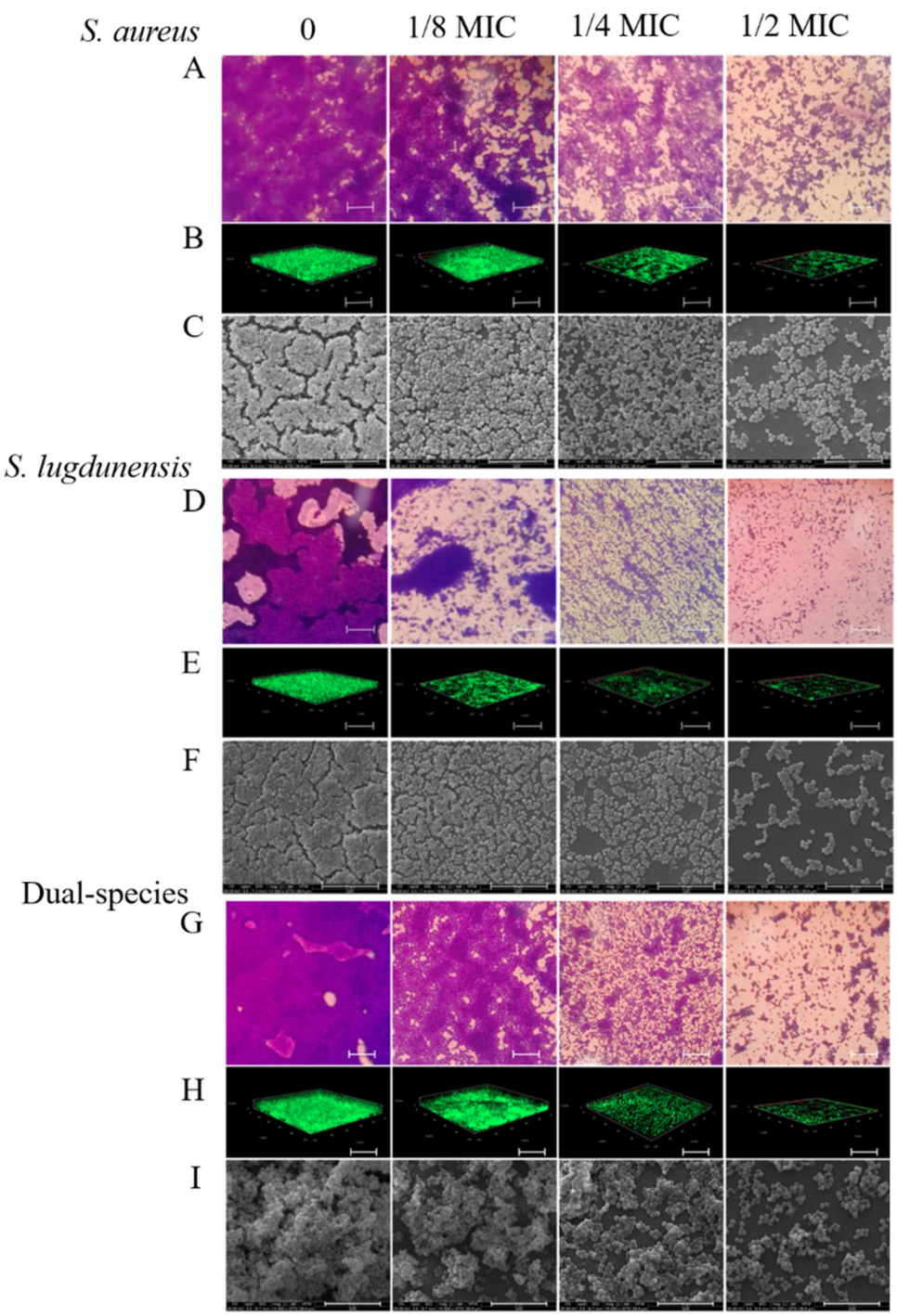

Fig. 4 Chelerythrine inhibited the biofilm formation of mono- and dual-species of *S. aureus* ATCC 25,923 and *S. lugdunensis* ATCC 700,328 on slides. The biofilms of dual-species formed on glass slides were inhibited by chelerythrine of different concentrations (0, 1/8 MIC, 1/4 MIC and 1/2 MIC). **a**, **d**, **g** Samples stained with crystal violet were observed by optical microscopy at the magnification of 40×(scale bar: 2.5 μm). **b**, **e**, **h** CLSM images. (scale bar: 10 μm) (**c**, **f**, **i**) Photographs of environmental scanning electron microscope (ESEM, magnification of 10,000×, scale bar: 10 μm)

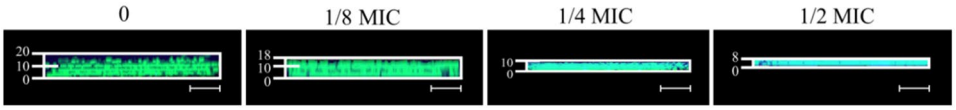

Fig. 5 Representative CLSM images assessing diffusion of gatifloxacin within dual-species of *S. aureus* ATCC 25,923 and *S. lugdunensis* ATCC 700,328 biofilms formed in the presence of chelerythrine. After dual-species biofilms were grown for 24 h supplemented without or with chelerythrine of different concentration, 0.08 mg mL^{-1} gatifloxacin was added into the medium, respectively. Following 5-h gatifloxacin diffusion, the biofilms were visualized using CLSM (scale bar: 10 μm). Biofilms were stained with SYTO 9 for biofilms (green) and the intrinsic fuorescence of gatifloxacin (blue)

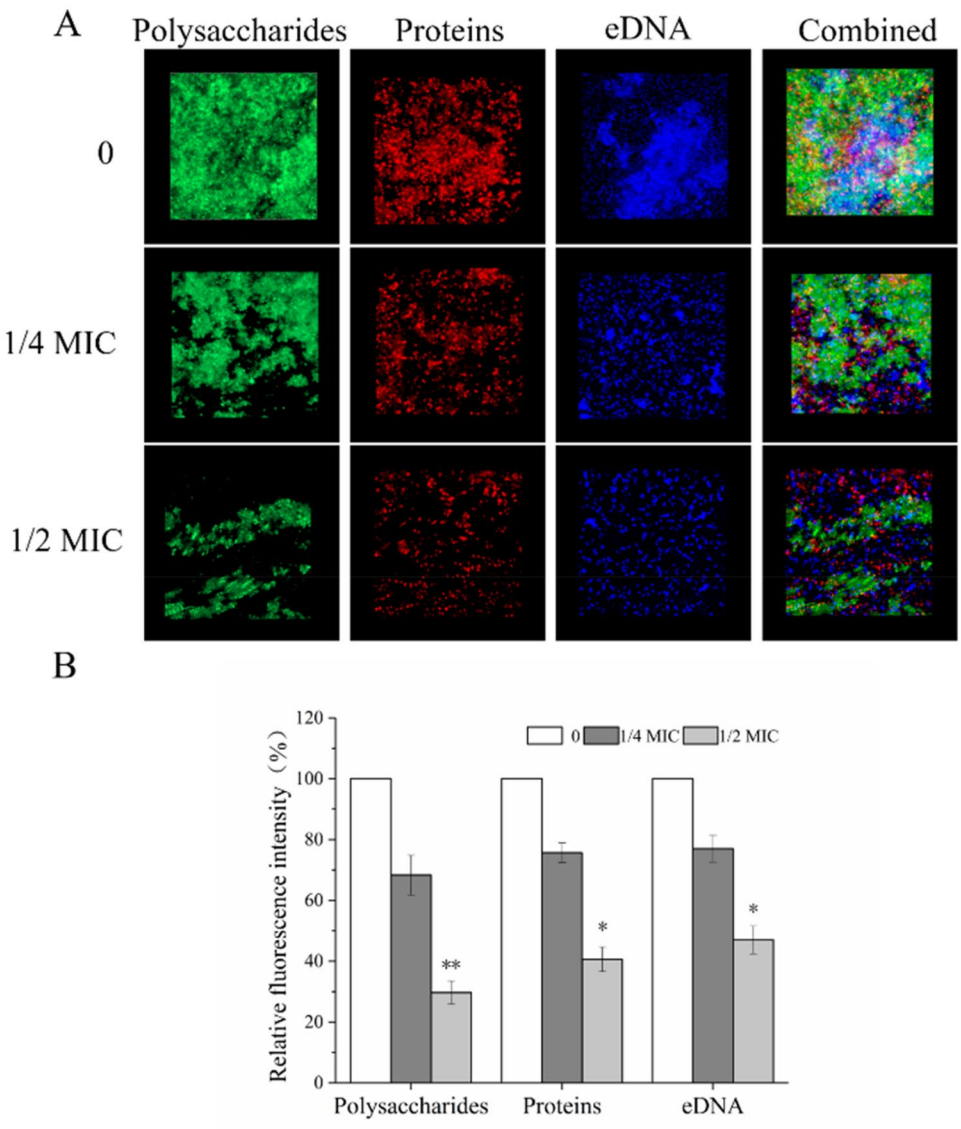

Fig. 6 CLSM images of biofilm composition (scale bar: 10 μm). Three fluorescent markers (SYPRO Ruby, WGA, and DAPI) were used to stain proteins, carbohydrates and eDNA of biofilm matrices, respectively. **a** CLSM images were examined at 63 × magnification. **b** The relative fluorescence intensity of each treatment group was calculated and plotted against that in untreated group using KS 400 version 3.0 software. Bars represent the standard deviation ($N = 6$), $^{**}P < 0.01$; *** $p < 0.001$

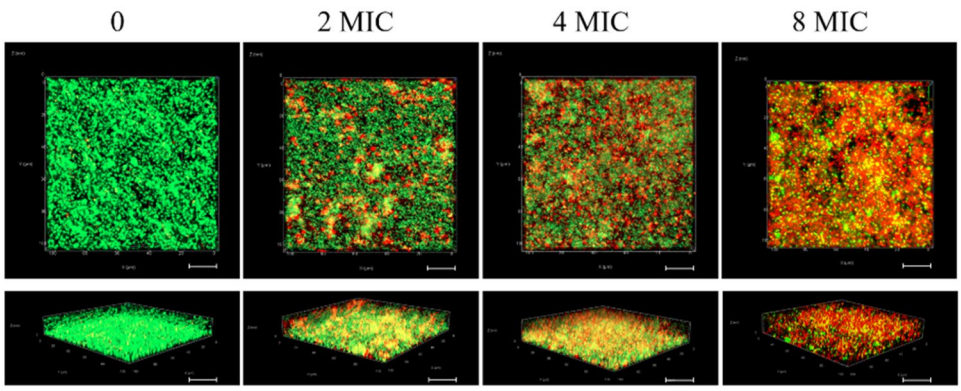

Fig. 7 Inactivation of chelerythrine against dual-species of *S. aureus* ATCC 25,923 and *S. lugdunensis* ATCC 700,328 within biofilms by CLSM (scale bar: 10 μm). Cells treated with chelerythrine at 0, 2 MIC, 4 MIC and 8 MIC, respectively

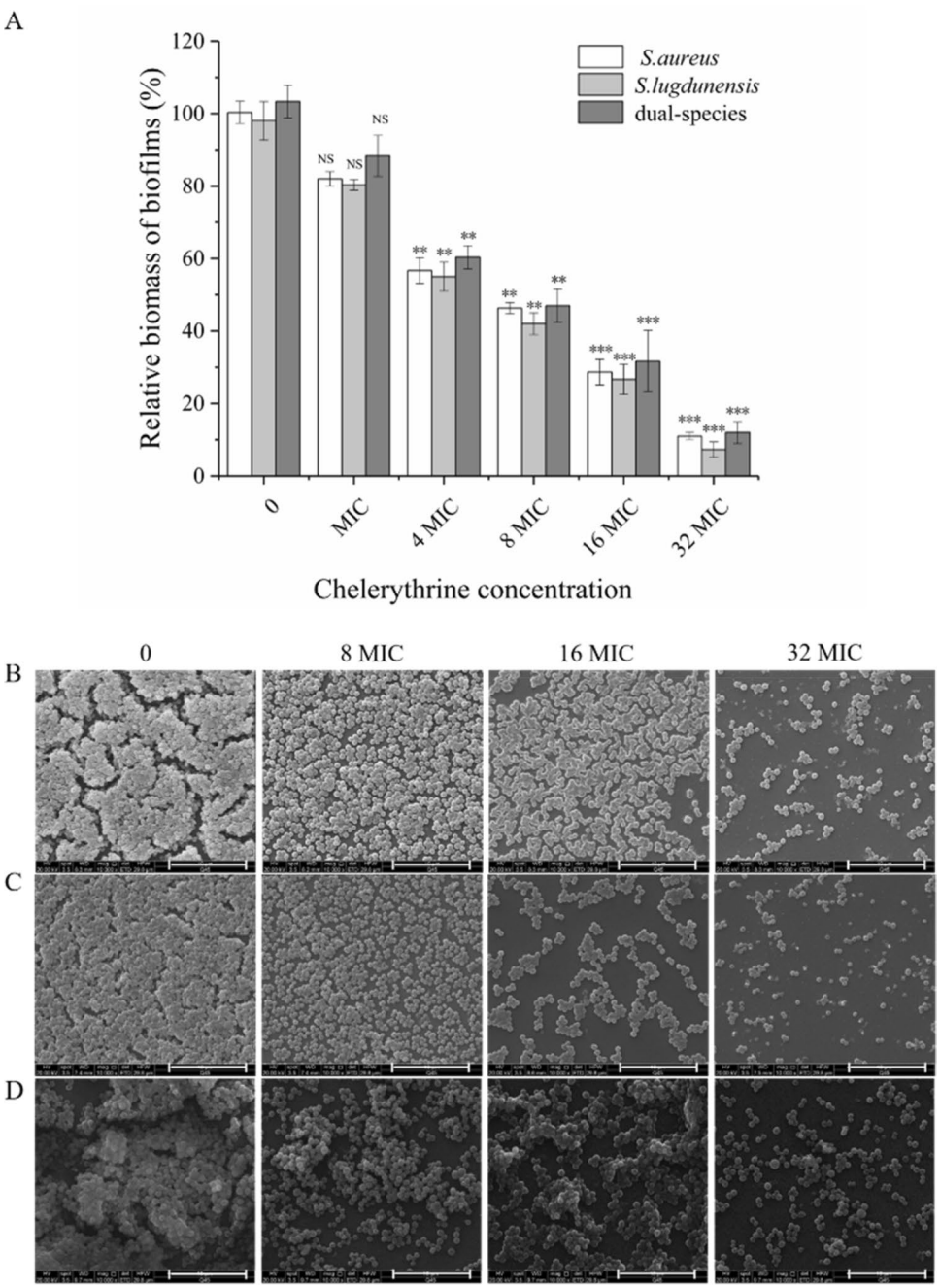

Fig. 8 Eradication effects of different concentration of chelerythrine on mono- and dual-species of *S. aureus* ATCC 25,923 and *S. lugdunensis* ATCC 700,328 mature biofilms. **a** The relative biomass of biofilm was assessed using crystal violet staining assay. Values represent the means of triplicate measurements. Bars represent the standard deviation ($n=3$). $^{*}P<0.05$; $^{**}P<0.01$; $^{***}P<0.001$; NS, not significant. **b**, **c**, **d** ESEM images of mono- and dual-species of *S. aureus* ATCC 25,923 and *S. lugdunensis* ATCC 700,328 mature biofilms after treatment with four concentrations of CHE (scale bar: 10 μm). Each field of vision was magnified 10 000×

Discussion

As an alternative antibiotic treatment, natural products are associated with lower antibiotic resistance than conventional drugs, and they are widely used in clinical settings. The current study investigated the antibacterial and antibiofilm effects of CHE, aiming to examine its antibiofilm effects against a commonly observed combination of bacterial species. CHE exhibited strong antibacterial effects against mixed cultures of *S. aureus* and *S. lugdunensis,* with an MIC value of 8 μg/mL. This is lower than a previous report that estimated its MIC at 0.156 mg/mL against *S. aureus* ATCC 25,923 and methicillin-resistant *S. aureus* (He et al. 2018). By comparison, Shen et al. reported that permeability of *S. aureus* ATCC 3101 cells was enhanced with exposure to 0.31 mg/mL cinnamaldehyde (its MIC) (Shen et al. 2015).

Surface colonization or adhesion, the initial stage of biofilm formation, enables planktonic microbial cells to attach the surfaces of medical devices. Our results showed that, in the adhesion stage, the antibiofilm effect of CHE on *S. aureus* and *S. lugdunensis* was to inhibit adhesion (Fig. 2). A CHE concentration of 4 μg/mL suppressed the adhesion of

S. aureus and *S. lugdunensis*. In contrast, a previous report showed that a zerumbone concentration of 128 µg/mL suppressed the adhesion of *S. aureus* ATCC 29,213 by 12.1% (Shin and Eom 2019).

We also investigated the inhibitory effects of CHE against *S. aureus-S. lugdunensis* biofilms by CVSA, ESEM, and CLSM. These methods showed a significant decrease of biofilm population following exposure to 1/4 MIC (2 µg/mL) CHE. In addition, CVSA revealed that CHE at 1/4 MIC was able to significantly suppress biofilm formation (Fig. 4g). Analogously, a previous study by Xu et al., showed that sub-MIC and MIC doses of punicalagin were also able to repress biofilm formation of *S. aureus* ATCC 29,213 (Xu et al. 2017). However, the biofilm of *S. aureus* was inhibited when the concentration of punicalagin was larger than 1/32 × MIC (7.8 µg/mL), while CHE inhibited dual-species biofilms at 1/2 MIC (4 µg/mL). We additionally demonstrated a clear increase in the diffusion of gatifloxacin within dual-species biofilms in the presence of 1/4 or 1/2 MIC CHE, suggesting that CHE increased biofilm permeability. Moreover, we used CLSM combined with three different fluorescent dyes to observe the matrix levels of biofilms exposed to CHE. The results suggested that 1/2 MIC CHE sharply inhibited biofilm formation via effects on polysaccharides, proteins, and eDNA (Fig. 6). These antibiofilm effects exhibited dose-dependency within 24 h of exposure, indicating that the three different matrix components strongly influenced biofilm development. Previous studies have also evaluated biofilm composition by performing CLSM image analysis on pathogens, including *S. aureus* and *Candida albicans* (Shin and Eom 2019).

In our study, CLSM images additionally showed the damage of cells encased within dual-species biofilms by CHE (Fig. 7). The rate of red/green fluorescence in dual-species culture treated with 4 MIC CHE was slightly higher than that of 2 MIC, indicating that the inactivating effect was dose-dependent. Interestingly, although biofilm cells exposed to 8 MIC CHE showed significant cell membrane damage, the existence of live cells located inside biofilm clusters suggests an important role of the three-dimensional organization of biofilms. This phenomenon is most likely due to reduced access of CHE to the bacteria. Similar CLSM assessment of antimicrobial effects on biofilms was conducted by Li et al. with dual-species biofilms of *Streptococcus mutans* ATCC 700,610 and *Streptococcus sanguinis* ATCC 10,556 (Li et al. 2014). The study suggested that nicotine causes damage to cells in dual-species biofilms.

Mature biofilm is associated with increased antibiotic resistance, and becomes difficult to remove (Salehzadeh et al. 2016; Montazeri et al. 2019). After verifying the antibiofilm activities of CHE, we evaluated its potential to eradicate biofilms. We found that CHE could eradicate ~ 90% of 24-h mature dual-culture biofilm at concentrations of 256 µg/mL (Fig. 8a). Meanwhile, In ESEM experiments (Fig. 8d) observing the influences of CHE on preformed flow-cell biofilms, we observed that 32 MIC efficiently reduced biofilms to either a monolayer of cells or a few attached cells, which was consistent with our CVSA results. In contrast, Shin et al. reported that in the case of preformed dual-species biofilms of *Candida albicans* ATCC 14,053 and *Staphylococcus aureus* ATCC 29,213, zerumbone only reduced antibiofilm activity by 39.4% compared with the control at concentrations of 500 µg/mL (Shin and Eom 2019).

In conclusion, our results indicate that CHE can inhibit the growth of dual-species biofilms formed by *S. aureus* and *S. lugdunensis*, and that CHE can also contribute to the bactericidal effect of other antibiotics on robust biofilm bacteria via its capacity to promote cell permeability. We note the following limitation of this study that is only a preliminary investigation, and further in vivo and clinical studies should be undertaken to verify the therapeutic beneficial effects of CHE on treatment of polymicrobial infections.

Acknowledgements This study was funded by the Key Research and Development Project of Shaanxi Province (2019JM-184), and the Industry Cultivation Project of Education Department of Shaanxi Provincial Government (18JC006, 18JC007).

Author contributions Design of the work was performed by WQ. Acquisition of data, analysis and interpretation, drafting and critical revision, approval of the final version and agreement to be accountable for the work were performed by ZS, YF, MY, TW, and YL.

Compliance with ethical standards

Conflict of interest The authors declare that they have no conflict of interest.

References

Dai J et al (2019) Prevalence and characterization of *Staphylococcus aureus* isolated from pasteurized milk in China. Front Microbiol 10:641. https://doi.org/10.3389/fmicb.2019.00641

de Oliveira A, Cataneli Pereira V, Pinheiro L, Moraes Riboli DF, Benini Martins K, Ribeiro de Souza da Cunha Mde L (2016) Antimicrobial resistance profile of planktonic and biofilm cells of *Staphylococcus aureus* and coagulase-negative *Staphylococci*. Int J Mol Sci 17 Doi: 10.3390/ijms17091423

Frank KL, Del Pozo JL, Patel R (2008) From clinical microbiology to infection pathogenesis: how daring to be different works for *Staphylococcus lugdunensis*. Clin Microbiol Rev 21:111–133. https://doi.org/10.1128/CMR.00036-07

Guo X et al (2019) Effect of D-cysteine on dual-species biofilms of *Streptococcus mutans* and *Streptococcus sanguinis*. Sci Rep 9:6689. https://doi.org/10.1038/s41598-019-43081-1

He N, Wang P, Wang P, Ma C, Kang W (2018) Antibacterial mechanism of chelerythrine isolated from root of *Toddalia asiatica (Linn) Lam*. BMC Complement Altern Med 18:261. https://doi.org/10.1186/s12906-018-2317-3

Hobley L, Harkins C, MacPhee CE, Stanley-Wall NR (2015) Giving structure to the biofilm matrix: an overview of individual

strategies and emerging common themes. FEMS Microbiol Rev 39:649–669. https://doi.org/10.1093/femsre/fuv015

Lee DH, Klinkova O, Kim JW, Nanjappa S, Greene JN (2019) A case series of *Staphylococcus lugdunensis* infection in cancer patients at an academic cancer institute in the United States. Infect Chemother 51:45–53. https://doi.org/10.3947/ic.2019.51.1.45

Li M, Huang R, Zhou X, Zhang K, Zheng X, Gregory RL (2014) Effect of nicotine on dual-species biofilms of *Streptococcus mutans* and *Streptococcus sanguinis*. FEMS Microbiol Lett 350:125–132. https://doi.org/10.1111/1574-6968.12317

Montazeri A, Salehzadeh A, Zamani H (2019) Effect of silver nanoparticles conjugated to thiosemicarbazide on biofilm formation and expression of intercellular adhesion molecule genes, icaAD, in *Staphylococcus aureus*. Folia Microbiol 65:153–160. https://doi.org/10.1007/s12223-019-00715-1

Olson ME, Ceri H, Morck DW, Buret AG, Read RR (2002) Biofilm bacteria: formation and comparative susceptibility to antibiotics. Can J Vet Res 66:86–92

Olszewska MA, Nynca A, Bialobrzewski I, Kocot AM, Laguna J (2019) Assessment of the bacterial viability of chlorine- and quaternary ammonium compounds-treated Lactobacillus cells via a multi-method approach. J Appl Microbiol 126:1070–1080. https://doi.org/10.1111/jam.14208

Oniciuc EA, Cerca N, Nicolau AI (2016) Compositional analysis of biofilms formed by *Staphylococcus aureus* isolated from food sources. Front Microbiol 7:390. https://doi.org/10.3389/fmicb.2016.00390

Qian W et al (2019) Antimicrobial activity of eugenol against carbapenem-resistant *Klebsiella pneumoniae* and its effect on biofilms. Microb Pathogenesis 139:103924. https://doi.org/10.1016/j.micpath.2019.103924

Rashed K, Ćirić A, Glamočlija J, Soković M (2014) Antibacterial and antifungal activities of methanol extract and phenolic compounds from *Diospyros virginiana L*. Ind Crops Prod 59:210–215. https://doi.org/10.1016/j.indcrop.2014.05.021

Ribeiro SM, de la Fuente-Nunez C, Baquir B, Faria-Junior C, Franco OL, Hancock RE (2015) Antibiofilm peptides increase the susceptibility of carbapenemase-producing *Klebsiella pneumoniae* clinical isolates to beta-lactam antibiotics. Antimicrob Agents Chemother 59:3906–3912. https://doi.org/10.1128/AAC.00092-15

Salehzadeh A, Zamani H, Langeroudi MK, Mirzaie A (2016) Molecular typing of nosocomial *Staphylococcus aureus* strains associated to biofilm based on the coagulase and protein A gene polymorphisms. Iran J Basic Med Sci 19:1325–1330. https://doi.org/10.22038/ijbms.2016.7919

Shen S, Zhang T, Yuan Y, Lin S, Xu J, Ye H (2015) Effects of cinnamaldehyde on *Escherichia coli* and *Staphylococcus aureus* membrane. Food Control 47:196–202. https://doi.org/10.1016/j.foodcont.2014.07.003

Shi C et al (2016) Antimicrobial activity and possible mechanism of action of citral against *Cronobacter sakazakii*. PLoS ONE 11:e0159006. https://doi.org/10.1371/journal.pone.0159006

Shin DS, Eom YB (2019) Efficacy of zerumbone against dual-species biofilms of *Candida albicans* and *Staphylococcus aureus*. Microb Pathog 137:103768. https://doi.org/10.1016/j.micpath.2019.103768

Tong SY, Davis JS, Eichenberger E, Holland TL, Fowler VG Jr (2015) *Staphylococcus aureus* infections: epidemiology, pathophysiology, clinical manifestations, and management. Clin Microbiol Rev 28:603–661. https://doi.org/10.1128/CMR.00134-14

Van der Waal SV, de Almeida J, Krom BP, de Soet JJ, Crielaard W (2017) Diffusion of antimicrobials in multispecies biofilms evaluated in a new biofilm model. Int Endod J 50:367–376. https://doi.org/10.1111/iej.12634

Van der Mee-Marquet N, Achard A, Mereghetti L, Danton A, Minier M, Quentin R (2003) *Staphylococcus lugdunensis* infections: high frequency of inguinal area carriage. J Clin Microbiol 41:1404–1409. https://doi.org/10.1128/jcm.41.4.1404-1409.2003

Xu Y et al (2017) Antimicrobial activity of punicalagin against *Staphylococcus aureus* and Its effect on biofilm formation. Foodborne Pathog Dis 14:282–287. https://doi.org/10.1089/fpd.2016.2226

Yang XJ et al (2012) In vitro antifungal activity of sanguinarine and chelerythrine derivatives against phytopathogenic fungi. Molecules 17:13026–13035. https://doi.org/10.3390/molecules171113026